

Localization of License Plate Number Using Dynamic Image Processing Techniques And Genetic Algorithms

G. Abo Samra, F. Khalefah

Abstract—In this research, a design of a new genetic algorithm (GA) is introduced to detect the locations of the License Plate (LP) symbols. An adaptive threshold method has been applied to overcome the dynamic changes of illumination conditions when converting the image into binary. Connected component analysis technique (CCAT) is used to detect candidate objects inside the unknown image. A scale-invariant Geometric Relationship Matrix (GRM) has been introduced to model the symbols layout in any LP which simplifies system adaptability when applied in different countries. Moreover, two new crossover operators, based on sorting, have been introduced which greatly improved the convergence speed of the system. Most of CCAT problems such as touching or broken bodies have been minimized by modifying the GA to perform partial match until reaching to an acceptable fitness value. The system has been implemented using MATLAB and various image samples have been experimented to verify the distinction of the proposed system. Encouraging results with 98.4% overall accuracy have been reported for two different datasets having variability in orientation, scaling, plate location, illumination and complex background. Examples of distorted plate images were successfully detected due to the independency on the shape, color, or location of the plate.

Index Terms—Genetic algorithms, image processing, image representations, license plate detection, machine vision, road vehicle identification, sorting crossover.

I. INTRODUCTION

THE detection stage of the LP is the most critical step in an automatic vehicle identification system [1]. A numerous research has been carried out to overcome many problems faced in this area but there is no general method that can be used for detecting license plates in different places or countries, because of the difference in plate style or design.

Manuscript received September 11, 2012. This paper was funded by the Deanship of Scientific Research(DSR), King Abdulaziz University, Jeddah, under grant No.(22-611- D1432). The authors, therefore, acknowledge with thanks DSR technical and financial support.

G. Abo Samra is an associate professor in the Faculty of Computing and Information Technology, King Abdulaziz University-Saudi Arabia (phone 00966-509189962; fax:00966-(02) 6951605;email: gabosamra@kau.edu.sa)

F. Khalefah is a lecturer in the Faculty of Computing and Information Technology, King Abdulaziz University (f.khalefah@gmail.com).

Copyright (c) 2012 IEEE. Personal use of this material is permitted. However, permission to use this material for any other purposes must be obtained from the IEEE by sending a request to pubs-permissions@ieee.org.

All the developed techniques can be categorized according to the selected features upon which the detection algorithm was based and the type of the detection algorithm itself. Color-based systems have been built to detect specific plates having fixed colors [2], [3], [4]. External-shape based techniques were developed to detect the plate based on its rectangular shape [5], [6], [7], [8]. Edge-based techniques were also implemented to detect the plate based on the high density of vertical edges inside it [9]-[11]. Researches in [12] and [13] were based on the intensity distribution in the plate's area with respect to its neighborhood where the plate is considered as Maximally Stable Extremal Region (MSER). Many researchers have combined different features in their systems [14], [15], [16], [17], [18]. The applied detection algorithms ranged from window-based statistical matching methods [18] to highly intelligent-based techniques that used neural networks [19], [20] or fuzzy logic [21]. GAs have been used rarely because of their high computational needs. Different researches have been tried at different levels under some constraints to minimize the search space of GAs. Researchers in [22] based their GA on pixel color features to segment the image depending on stable colors into plate and non plate regions, followed by shape dependent rules to identify the plate's area. Success rate of 92.8% was recorded for 70 test-samples. In [23], GA was used to search for the best fixed rectangular area having the same texture features as that of the prototype template. The used technique lacks invariability to scaling because fixed parameters have been used for the size of the plate's area. In [24], GA was used to locate the plate vertically after detecting the left and right limits based on horizontal symmetry of the vertical texture histogram around the plate's area. The drawback of this method is its sensitivity to the presence of model identification text or other objects above or below the vehicle which can disturb the texture histogram. GA was used in [25] to recognize the LP symbols not to detect the LP. Another group of researchers tried to manipulate the problem from the texture perspective to differentiate between text and other image types [26], [27]. The main drawback of these segmentation techniques was their intensive computational demand and also sensitivity to the presence of other text such as bumper stickers or model identification.

Detecting license text and at the same time distinguishing it from similar patterns based on the geometrical relationship between the symbols constituting the license numbers is the

selected approach in this research. Consequently, a new technique is introduced in this paper which detects LP symbols without using any information associated with the plate's outer shape or internal colors to allow for the detection of the license numbers in case of shape or color distortion either physically or due to capturing conditions such as poor lighting, shadows and camera position and orientation. To search for the candidate objects and to allow for tolerance in the localization process, a new genetic algorithm has been designed with a new flexible fitness function. Image processing is carried out at first to prepare for the GA phase. A complete overview of the system is given in Section II. Image processing stages are presented in Section III. In Section IV, GA formulation is demonstrated. In Section V, modifications to the GA stage to overcome most of the problems associated with CCAT are summarized. Finally, the results are discussed in section VI.

II. SYSTEM OVERVIEW

In this section, an overview of the system is introduced. The proposed system is composed of two phases: image processing phase and GA phase. Each phase is composed of many stages. The flowchart in Fig. 1 depicts the various image processing stages that finally produce image objects to the GA phase. GA selects the optimum LP symbol locations depending on the input GRM that defines the geometrical relationships between the symbols in the concerned LP.

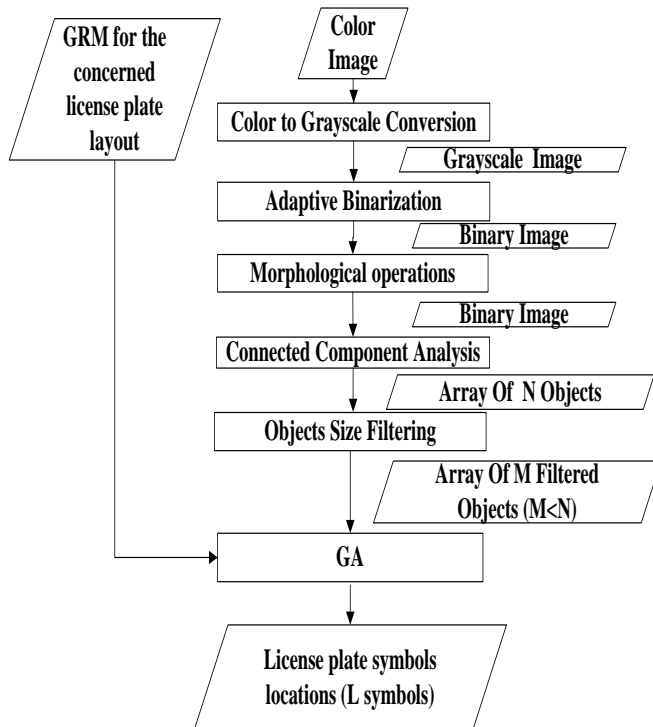


Fig. 1. The system's overall flowchart for the localization of the LP symbols.

III. IMAGE PROCESSING PHASE

In this phase, an input color image is exposed to a sequence of processes to extract the relevant two dimensional objects that may represent the symbols constituting the LP. These processes that are carried out in different stages, as depicted in Fig. 1, will be presented in the following subsections.

A. Color to grayscale conversion

The input image is captured as a color image taking into account further processing of the image to extract other information relevant to the concerned vehicle. Color (RGB) to grayscale (gs) conversion is performed using the standard NTSC method by eliminating the hue and saturation information while retaining the luminance as follows:

$$gs=0.299*R+0.587*G+0.114*B \quad (1)$$

Fig. 2 shows an example of the output of this stage that will be used as input to the next stage.



Fig. 2. Converted grayscale image.

B. Gray to binary using a dynamic adaptive threshold

Converting the input image into a binary image is one of the most sensitive stages in localizing LPs due to spatial and temporal variations encountered in the plate itself and the environment around it resulting in several illumination problems. Hence binarization of the image according to a fixed global threshold is not suitable to overcome these problems. In our system, a local adaptive method based on the techniques described in [28] has been implemented to determine the threshold at each pixel dynamically depending on the average gray level in the neighborhood of the pixel. A simple yet effective rule has been adopted to differentiate between foreground and background pixels. If the pixel intensity is higher than 90% of the local mean it is assigned to the background; otherwise it is assigned to the foreground. The 10% offset below the mean is chosen experimentally to minimize the sensitivity to fluctuations in illumination. The size of the window used to calculate the threshold for each pixel is selected according to the image resolution and the expected size of the license symbols. A 30x30 window has been applied on the first set of image samples used in this research, which resulted in a high accuracy rate in different illumination conditions as will be presented in the results section. Although some images can be binarized successfully using Otsu's global threshold method [29] as shown in Fig. 3(a), others as that shown in Fig. 3(b) may produce incorrect results as shown in Fig. 3(c). On the other hand, local adaptive binarization will give satisfactory output as shown in Fig. 3(d) for the same image in Fig. 3(b).

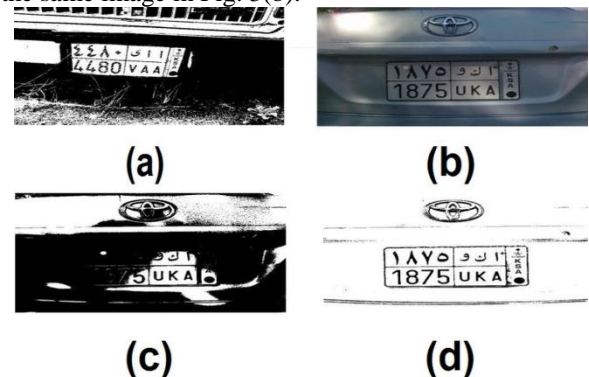


Fig. 3. (a) Converted binary image for image in Fig. 2, using Otsu's method, (b) Car image with variable illumination, (c) output when using Otsu's method for image in (b), (d) output when applying local adaptive threshold method for the same image in (b).

C. Morphological operations

Morphological operations such as dilation and erosion are important processes needed for most pattern recognition systems to eliminate noisy objects and retain only objects expected to represent the targeted patterns. In LP detection, closing operation (dilation followed by erosion) is performed to fill noisy holes inside candidate objects and to connect broken symbols. On the other hand, opening (erosion followed by dilation) is applied to remove objects that are thinner than the LP symbols. In our system, closing is applied to fill spaces that break the bodies of symbols using a 3-pixel-disk element in the first experiment. This process is very important especially for the recent Saudi LP layout where a light gray watermark is used for authentication purposes. This watermark becomes white after the binarization process and breaks down most of the bodies of the LP symbols as shown in Fig. 4(a). Fig. 4(b) shows the output after applying closing. For non Saudi LP images, a disk radius of less length is used to prevent filling the spacing between the LP symbols. Removal of thin objects is performed in the size filtering stage.

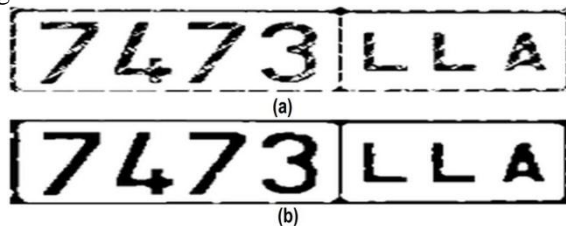


Fig. 4. Morphological closing using 3-pixel disk-element (a)Input Binary Image, (b)Image after closing operation.

D. Connected Component Analysis (CCA) and objects extraction

CCA is a well known technique in image processing that scans an image and groups pixels in labeled components based on pixel connectivity [30]. An 8-point CCA stage is performed to locate all the objects inside the binary image produced from the previous stage. The output of this stage is an array of N objects. Fig. 5 shows an example of the input and output of this stage.

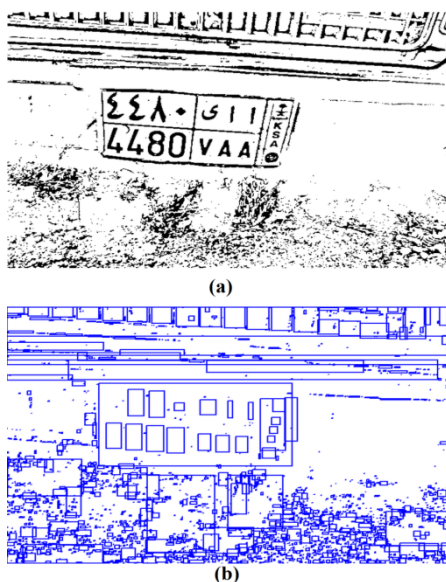


Fig. 5. CCA example: (a) Input image, (b) output objects ($N=2287$).

E. Size filtering

The objects extracted from the CCA stage are filtered on the basis of their widths W_{obj} and heights H_{obj} such that the dimensions of the LP symbols lie between their respective thresholds as follows:

$$W_{\min} \leq W_{obj} \leq W_{\max} \quad \text{and} \quad H_{\min} \leq H_{obj} \leq H_{\max} \quad (2)$$

Where H_{\min} and W_{\min} are the values below which a symbol cannot be recognized (8 pixels for example) and W_{\max} can be set to the image width divided by the number of symbols in the license number. H_{\max} is calculated as W_{\max} divided by the aspect ratio of the used font. The ranges of these values can be narrowed in the case of a mounted camera to speed up the process of detection but for a moving camera, the ranges depend on the required object to camera distance range. The output of this stage is an array of M objects. An example for the output of this stage is given in Fig. 6 after applying size filtering on the objects shown in Fig. 5(b).

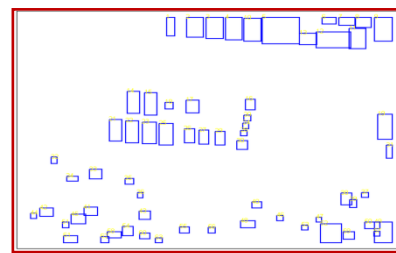


Fig. 6. M objects (64) output after size filtering of the N objects in Fig. 5(b).

IV. GA PHASE

In the following sections, the formulation of the GA phase to resolve the 2D compound object detection problem will be introduced in details, indicating the encoding method, initial population setup, fitness function formulation, selection method, mutation and crossover operator design and parameters setting.

A. Chromosome encoding

Encoding of a compound object such as the LP is accomplished based on the constituting objects inside it. Since the next step after plate detection is to recognize the license number, hence the main symbols identifying the plate number should be included as a minimum. In the case of the recent Saudi LP, for example, there are 4 Arabic digits and 3 English letters. Other symbols in the LP can be added to extend the representation for more layout discrimination if needed. In our experiments, only the 7 symbols (4 digits and 3 letters) are used to detect the LP number. Hence for the Saudi layout, as an example, the chromosome will be composed of 7 genes as shown in Fig. 7. An integer encoding scheme has been selected where each gene i is assigned an integer j which represents the index to one of the M objects output from the size filtering stage. The information that will be used for each object j is as follows:

- The upper left corner coordinates (X, Y) of the rectangle bounding the object.
- The height (H) and width (W) of the rectangle bounding the object.

gene number (i):	1	2	3	4	5	6	7
object index (j)	3	1	5	7	11	2	15

Fig. 7. A chromosome of 7 genes for the representation of the Saudi LP.

B. Defining the fitness function

The proposed fitness is selected as the inverse of the calculated objective distance between the prototype chromosome and the current chromosome. Before clarifying how the objective distance is measured, we will show first how the geometric relationships between the objects inside a compound object are represented, followed by a discussion of parameter adaption in case of various LP detection layouts.

Compound object representation

For any two objects, we will use two types of geometrical relationships that can be defined as follows:

1. Position relationship:

The position relationship will be represented by the relative distances between the bounding boxes of the two objects in the X and Y directions.

2. Size relationship:

The size relationship will be represented as the relative differences in their bounding boxes' heights and widths.

In the above relationships, relativity is achieved by dividing on the height or width of the first object depending on which is more stable for practical reasons although it is logically to divide differences in heights on height and differences in widths on width to compensate for scale changes in the general case. For most LPs (see Appendix), the heights of symbols are almost equal for both digits and letters while some symbols have different widths than others. Hence, normalized relationships between any two objects can be based on the height of the first object.

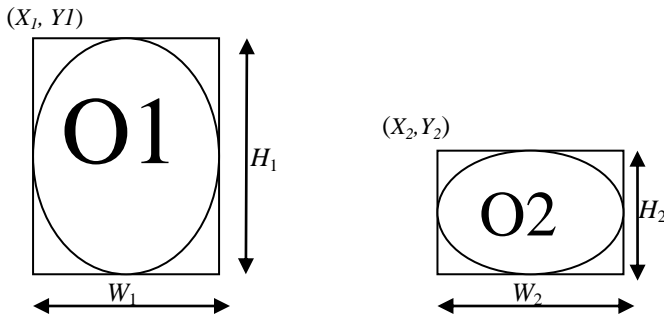


Fig. 8. The layout of two objects O1 and O2.

Considering the two objects O1 and O2 shown in Fig. 8, the position relationship is defined in the two directions by the following formulas:

$$RX_{2,1} = (X_2 - X_1)/H_1 \quad (3)$$

$$RY_{2,1} = (Y_2 - Y_1)/H_1 \quad (4)$$

The size relationship is defined by the following formulas:

$$RH_{2,1} = (H_2 - H_1)/H_1 \quad (5)$$

$$RW_{2,1} = (W_2 - W_1)/H_1 \quad (6)$$

The above representation, although preserves the geometric relationships between the rectangles bounding the objects, it does not represent the objects' shapes because they are unknown in case of an unknown plate. Only the aspect ratio for fixed width-fonts can be added for the first object as follows:

$$AS_j = W_j/H_j. \quad (7)$$

To generalize the representation for any compound object composed of L objects, only $4(L-1)$ relationships will be required in addition to the aspect ratio for the first object.

For example, if we consider the Saudi LP shown in Fig. 9, 25 relationships will be required to represent the layout of the seven lower license symbols (4 Arabic digits and 3 English letters) ($L=7$).



Fig. 9. Saudi LP with rectangles bounding the represented symbols.

In general, for L -symbol LP we will need $(4(L-1)+1)$ values to represent the license number. Placing the values of the different relationships in one matrix (excluding the aspect ratio), produces what we called the geometric relationships matrix GRM. Table I presents the values of the GRM for the Saudi LP shown in Fig. 9; where the variable j denotes the index of each symbol from left to right.

TABLE I: GRM VALUES FOR THE SAUDI LP.

j	1	2	3	4	5	6
$RX_{j+1,j}$	0.615	0.615	0.615	0.77	1	1
$RY_{j+1,j}$	0	0	0	0.2	0	0
$RW_{j+1,j}$	0	0	0	-0.08	0	0
$RH_{j+1,j}$	0	0	0	-0.5	0	0

To adapt the system for a different LP layout either in the same country or in a different one, a different GRM matrix can be simply defined.

Objective Distance (OD) and Fitness Formulation

Considering the distance between the prototype chromosome p , corresponding to the input GRM, and any chromosome k , five distance values can be defined as follows:

$$\Delta RX_{k,p} = \sum_{j=1}^{L-1} \left| (RX_{j+1,j})_k - (RX_{j+1,j})_p \right| \quad (8)$$

$$\Delta RY_{k,p} = \sum_{j=1}^{L-1} \left| (RY_{j+1,j})_k - (RY_{j+1,j})_p \right| \quad (9)$$

$$\Delta RW_{k,p} = \sum_{j=1}^{L-1} \left| (RW_{j+1,j})_k - (RW_{j+1,j})_p \right| \quad (10)$$

$$\Delta RH_{k,p} = \sum_{j=1}^{L-1} \left| (RH_{j+1,j})_k - (RH_{j+1,j})_p \right| \quad (11)$$

$$\Delta AS_{k,p} = |AS_k - AS_p| \quad (12)$$

Clearly, these distance values will be considered as the objective distance functions in our GA problem, which should be minimized.

Combining the five objective distance functions into one global objective distance function $OD_{k,p}$ that represents the distance between any chromosome k and the prototype chromosome p , is performed through the following formula:

$$OD_{k,p} = w_x \Delta RX_{k,p} + w_y \Delta RY_{k,p} + w_h \Delta RH_{k,p} + w_w \Delta RW_{k,p} + w_{as} \Delta AS_{k,p} \quad (13)$$

Where w_x , w_y , w_h , w_w and w_{as} are weighting parameters that should be given values according to the problem under consideration.

Since, as stated in the literature, the fitness is a function that should be maximized, hence the fitness of chromosome k (Fit_k) can be related to the global objective distance function as follows:

$$Fit_k = -OD_{k,p} \quad (14)$$

Adaption for the LP detection problem

The previous formulation can be used for the representation of a compound object consisting of a group of smaller objects and can be used to locate the compound object in an image given that its GRM values are nearly fixed. This formulation has an advantage of overcoming scaling effect. It can also overcome orientation variability either by aligning the compound objects to a certain direction line or by taking projection parameters into account in the original formulation. Although in our formulation, orientation independency is not taken into consideration, detection of plates having different orientations has been achieved as will be shown in the results section due to the flexible range of accepted fitness (or objective distance) values.

An important issue that should be considered when adapting the previous model for LP detection is the variable nature of the internal components (letters or digits) in an unknown plate. In other words, the symbols inside an unknown plate can vary in size and/or spacing. Hence representation of an unknown plate license number will require some adaptation of the general model according to the nearly stable features of the symbols used in the plate and the relative spacing between them. Referring to the Appendix which contains 25 LPs for 25 different countries in different continents, adaption can be carried out as follows:

- Since, in some LP layouts especially in Arabic countries, the symbols used can differ greatly in their widths, hence the term corresponding to the relative width can be neglected by setting the weighting parameter w_w to zero.
- The aspect ratio of the starting letter is not fixed in case of variable width fonts and also may be changed due to perspective mapping. Hence, a range of accepted values of the aspect ratio can be imposed in the size filtering

stage based on the characteristics of the used font. This means that the parameter w_{as} may also be set to zero.

- The values of the parameters w_x , w_y , w_h can be selected to reflect the importance of each term as follows.
 - Since the license symbols are almost horizontally aligned, then w_y will be given the highest value (e.g. 4).
 - For fixed height fonts, w_h can be as high as w_y (e.g. 4), but for the general case its value can be selected lower than w_y (in case of Arabic letters) because horizontal alignment is more important than height changes.
 - The term $\Delta RX_{j,p}$ corresponds to the horizontal distance between LP symbols which can vary for variable width fonts; hence its weighting parameter w_x will be given the lowest value (e.g. 1).
- Hence, the objective distance function for the detection of the LP number for almost all LPs (Arabic digits and English letters) shown in Appendix, can be put in the following form:

$$OD_{k,p} = \Delta RX_{k,p} + 4\Delta RY_{k,p} + 4\Delta RH_{k,p} \quad (15)$$

It should be recorded here that the selection of the weighting parameters affects and guides the genetic search space during the production of new generations and hence affects both speed and accuracy of the overall system.

Finally, by substituting from 15 into 14, the formula for the fitness of a chromosome k (Fit_k) is given as follows:

$$Fit_k = -\Delta RX_{k,p} - 4\Delta RY_{k,p} - 4\Delta RH_{k,p} \quad (16)$$

C. The selection method

In our system, the Stochastic Universal Sampling (SUS) method has been adopted for the selection of offspring in the new generation. In SUS method [31], each individual is mapped to a continuous segment of a line equal in size to its fitness as in roulette-wheel selection. Then, a number of equally spaced pointers are placed over the line depending on the percentage of individuals to be selected. In our system, individuals of ninety percent of the population size (0.9 Z) are selected to be exposed to mutation and crossover operators.

D. Mutation operators

Mutation is needed because successive removal of less fit members in genetic iterations may eliminate some aspects of genetic material forever. By performing mutation in the chromosomes, GAs ensure that new parts of the search space are reached to maintain the mating pool variety [32]. We have implemented two types of interchangeably used mutation operators; substitution operator and swap operator as follows:

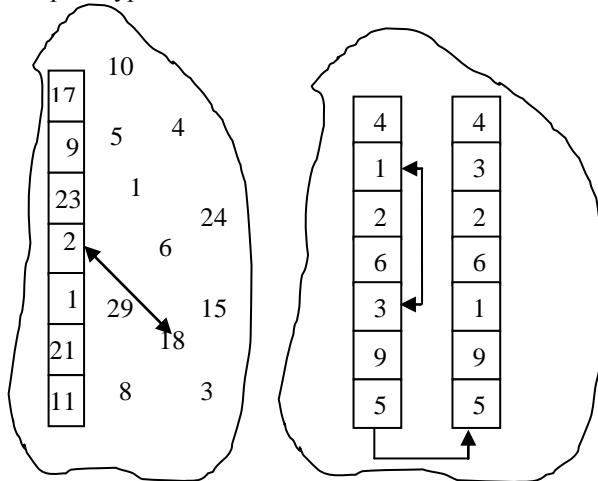
Substitution operator

In this type of operators, a random position in the chromosome is selected and the corresponding allele is changed by a new random object from the M available objects.

The new object should be legitimate which means it does not belong to the current mutated chromosome. Fig. 10(a) shows an example of the application of this operator.

Swap operator

In this operator, we implemented the reciprocal exchange mutation that selects two genes randomly and swaps them as shown in Fig. 10(b). This operator has the advantage of rearrangement of the mutated chromosome in a way that may improve its fitness by reordering of the internal objects to match the prototype's order.



(a) Substitution operator. (b) Swap operator. Fig. 10. Examples for the used mutation operators.

E. Crossover operator

There are many methods to implement the crossover operator. For instance, single point crossover, two point crossover, n-point crossover, uniform crossover, three parent crossover and, alternating crossover [33], etc. These operators are not suitable for our problem because the resultant children will not be valid because of repeated genes that may be produced in the generated chromosomes. Also, if we prevent repetition, the resultant children's fitness will be enhanced slowly because of the randomness of these mechanisms. An alternative solution is to design a suitable crossover operator that insures enhancement of the generated offspring. Since, in case of LP detection problem, GA is used to search for a sequence of objects having nearly the same y-position and placed in order according to their x-positions, then the problem can be gradually solved by dividing the recombined chromosomes' objects according to their y-positions into two groups and then sorting each group (constituting a chromosome) according to the x-positions. Following the above discussion, we propose a new crossover method that depends mainly on sorting as follows:

1. The two parent chromosomes are combined into one longer array *Carray* that includes a number *NC* of non repeated genes as shown in Fig. 11 (a, b, c). The underlined gene number indicates its repetition and that only one copy of it will be transferred to *Carray*.
2. The genes inside *Carray* are sorted in ascending order according to the *Y*-coordinate of the object corresponding to each gene as shown in Fig. 11(d).

3. *Carray* is scanned from left to right starting from index 1 to *L*, to construct the first child giving it the first *L* genes as shown in Fig. 11(e).
4. *Carray* is scanned from left to right starting from index $NC-L+1$ to NC , to construct the second child giving it the last *L* genes as shown in Fig. 11(f).
5. Each child is sorted in ascending order according to the *X*-coordinate of each gene's object to produce the final shape of each child as shown in Fig. 11 (g, h) respectively.

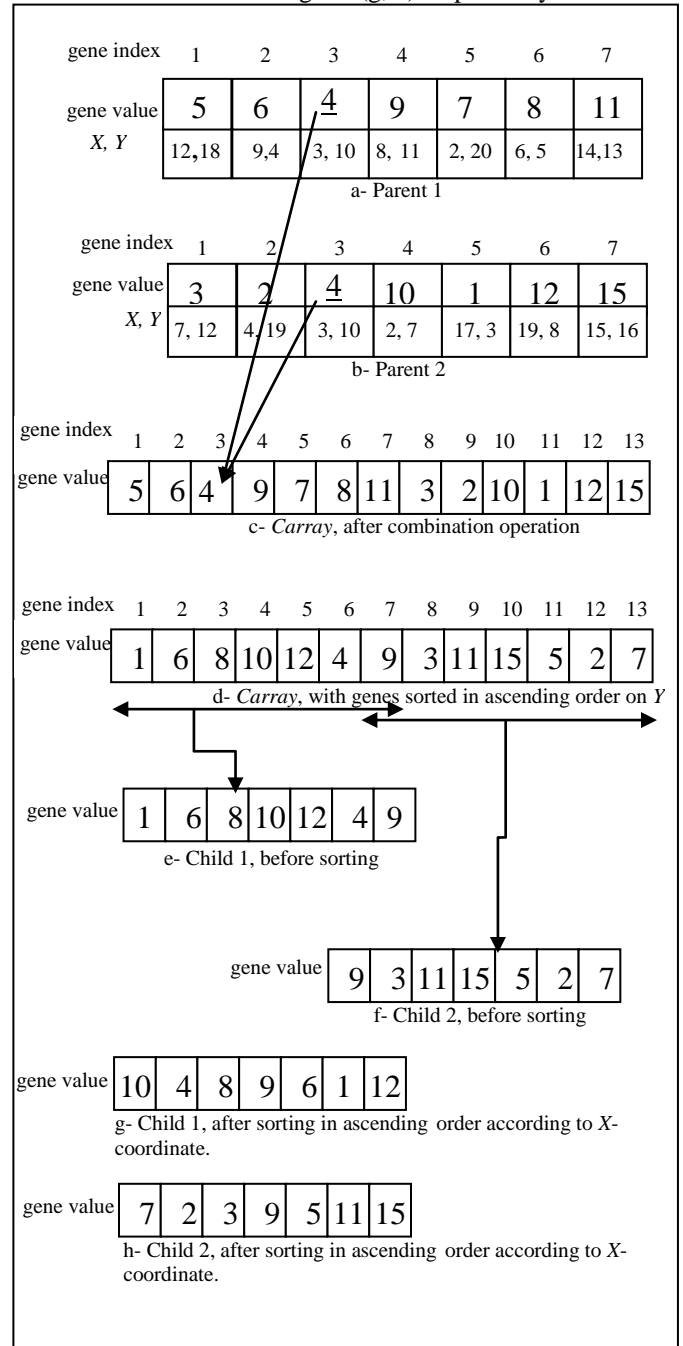


Fig. 11. The proposed crossover operator steps.

Since this operator starts by combining objects without repetition (Union operation) and then performs Sorting and Partitioning followed by Sorting, we can call it USPS crossover to differentiate it from the known sorting crossover. Although sorting requires a significant time, the overall time is

reduced because the number of generations needed to reach to the stopping criteria is sharply decreased as shown in Fig. 12(b) compared to the case of 2-point random crossover shown in Fig. 12(a). The offspring of the random crossover are repaired by replacing repeated genes by non repeated ones randomly. Fig. 13 presents another 2 examples in which the USPS crossover outperforms the 2-point random crossover.

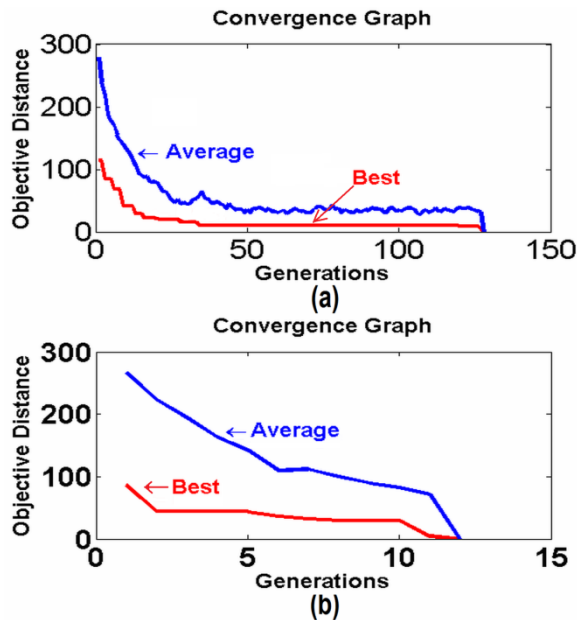


Fig. 12. Objective Distance (OD) convergence graphs for the image in Fig. 2, using 2-point random crossover in (a) and USPS crossover in (b).

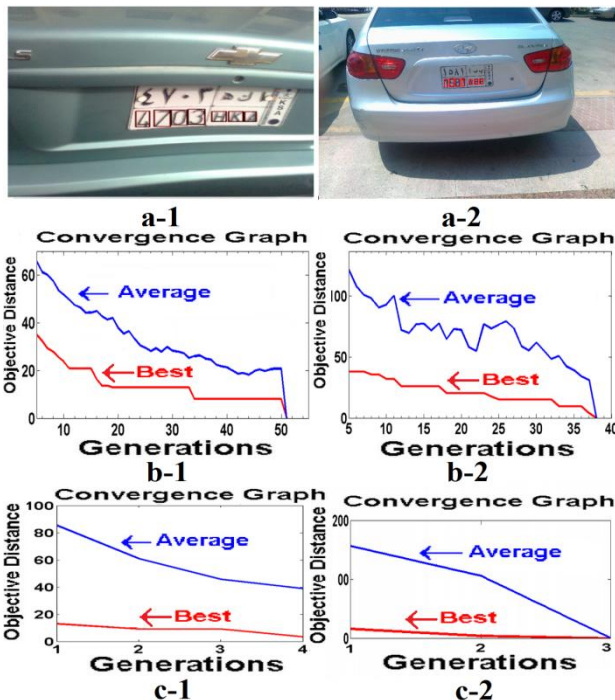


Fig. 13. Objective Distance (OD) convergence graphs for the two images shown in a-1 and a-2 with random crossover in b-1 and b-2 and USPS crossover in c-1 and c-2 respectively.

Trying other types of crossover operators may give better results than the tested one, but we are sure that our proposed crossover will outperform them because it generates the final solution almost in one step if the solution genes are included

in the original parents. Moreover, it gives excellent intermediate solutions by clustering the objects based on their y-positions and sorts them based on x-positions.

F. Replacement strategy

Many replacement strategies are used in case of replacing only a portion of the population between generations. The most common strategy is to probabilistically replace the less fit individuals in the previous generation. In elitist strategy the best fit individuals of the previous generation are appended to the current population [34]. In our proposed system, the best 10% of the parents are selected and appended to the offspring (90%) to produce the new generation (100%).

G. Stopping criteria

The GA stops if one of the following conditions is met:

- 1-The best chromosome's objective distance (OD) is less than 5. (This value is found by trial and error).
- 2-The average objective distance (AOD) is not improved for 6 successive generations. In this case, the chromosome having minimum objective distance can be accepted if it is less than 8. This maximum limit will affect the allowable angle range for the detected license numbers as shown in Table II.

TABLE II: OBJECTIVE DISTANCES (OD) FOR PLATES INCLINED AT DIFFERENT ANGLES [A: -30° TO +45°].

A = -30°	A = -20°	A = 10°	A = 20°	A = 45°
OD=16.6	OD=11.2	OD=6.4	OD=11.2	OD=19.2

- 3-The number of generations N_{gen} reaches to the maximum number of generations $MaxN_{gen}$ (set to 20).

H. Parameters setting

The population size (Z) is selected dynamically according to the formula developed in [34] as follows:

$$Z = 1.65 \times 2^{(0.21 * blength)} \quad (17)$$

Where $blength$ is the length of the chromosome in case of binary encoding. In case of integer encoding, for L genes and M objects, we substitute for $blength$ by:

$$blength = L (\log_2(M)) \quad (18)$$

Although formula (17) is driven in 1989, it speeds up the convergence of the GA as shown in Fig. 14 ($Z=845$, $N_{gen}=5$) compared to the graph in Fig. 12(b) with static population size ($Z=500$, $N_{gen}=12$) for the same image in Fig. 2.

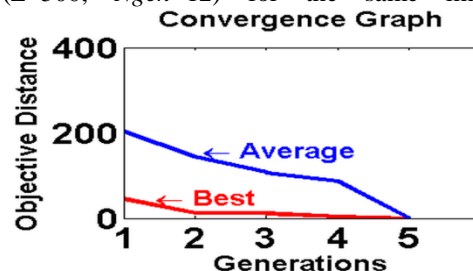


Fig. 14. OD convergence graph for dynamic population size ($Z=845$).

V. MINIMIZING CCAT PROBLEMS

The main drawback of all systems relying on CCAT is the sensitivity to negative or positive noise that may cause some symbols to be connected to other objects or broken into smaller objects. Connectivity is also affected by many causes such as bullets, dirt, aging, occlusion, shadows, or due to image processing operations like dilation and erosion. The effect of connected symbols either to their neighbors or to the frame of the LP is the introduction of high objective distance when matched with the corresponding GRM. This surely, will cause the system to select another near symbol or to report absence of LP in the current image. The same is said in the case of broken bodies, where a large error is detected in the relative width/height terms. The proposed solution for this problem is to introduce a new argument in the genetic algorithm which indicates the number of symbols to skip (NS) during the evaluation of the objective distance. This number is initialized to zero in the first run of the GA and according to the optimum OD threshold value (ODT), a decision is made either to accept the selected chromosome or to increase the NS argument and execute a further run of the GA. Depending on the number of LP symbols (L) under consideration, the skipping number NS can reach to a maximum value given that $L-NS \geq 3$. If NS is greater than zero then NS random numbers having values between 1 and L are generated inside the OD evaluation function, and the corresponding gene error distances are skipped. Surely, these random numbers should be stored in separate fields associated with each chromosome as shown in Fig. 15.

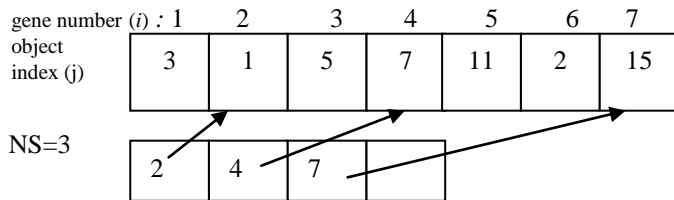


Fig. 15. An example for the locations of skipped genes stored in separate fields associated with each chromosome.

Finally if the OD threshold (ODT) test is met, the location and size of the skipped symbols are estimated based on the GRM matrix and the non skipped symbols using some geometrical rules. The flow chart illustrating the logic of these steps is shown in Fig. 16. The proposed modification has solved many problems happening due to static causes like dirt and pullets or dynamic causes like shadows, lighting and even blurring caused by camera movement because it gives another dimension for solving the LP detection problem by expecting locations of occluded or distorted symbols. Fig. 17 shows an example of two images from two different layouts (Saudi and Greece) containing touching symbols in two different ways which have been correctly detected after GA modification.

Another simple yet very effective modification is done to cluster objects based on their x-positions by introducing an alternate USPS crossover which works interchangeably with the described one but it sorts the unified parents based on x-positions first instead of y and hence after the partitioning step, children will be already sorted based on x-positions. This modification speeds up the GA phase in case of large number of objects output from CCAT by about 20% than without it.

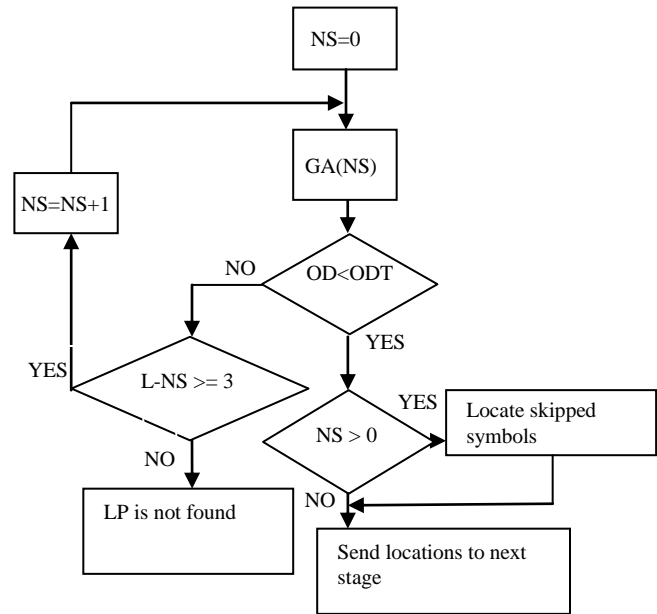


Fig. 16. Flowchart for detecting LP's symbols in case of touching and broken symbols.



Fig. 17. Examples for locating symbols touching the digit's bounding box (digit '1' in (a)) and touching each other (last two digits in (b)).

VI. RESULTS AND DISCUSSION

The proposed system has been implemented using MATLAB. Two experiments were carried out. The first experiment was done on a Saudi LP dataset composed of 800 car images acquired at various camera-to-object relative positions in different lighting conditions. To compare our results, we consider the work published in [9], because it used an annotated database which allows us to precisely experiment our technique on the same dataset. Hence, the second experiment is performed on the same 335 image samples used by [9] that are available in [35] for Greece LPs (shown in the Appendix table (column 2 row 2)). This database includes four datasets: Day (color images large sample), Day (close view), Day (with shadows), and Shadows in plate. Only one standard Greece LP image is used to construct the GRM matrix to adapt our system on this different layout as shown in Table III. Noting that zero values in the 2nd, 3rd, 4th rows mean same base line, fixed width and fixed height respectively for all the symbols used in the defined plate. In both experiments, the third row is neglected by setting the weighting parameter w_w to zero due to violation of the fixed width for the letter 'I' and digit '1'. Results of our experiments are summarized in the first three rows in Table IV; where false positive (FP) means assigning incorrect locations to LP symbols. Surely the remaining undetected cases are false negative (FN) cases where each image includes an LP but the ODT test is not met

for all combinations of objects in the tested images. Results for the two experiments done by [9] are shown in the 4th and 5th rows in Table IV. The first experiment done by [9] is performed on the same 335 samples in [35]. The second experiment is done after appending an enlarged version of the largest 113 images in the first experiment to its 335 samples.

TABLE III: GRM FOR THE GREECE LP.

j	1	2	3	4	5	6
$RX_{j+1,j}$	0.8	0.8	1.55	0.8	0.8	0.8
$RY_{j+1,j}$	0	0	0	0	0	0
$RW_{j+1,j}$	0	0	0	0	0	0
$RH_{j+1,j}$	0	0	0	0	0	0

TABLE IV: RESULTS OF OUR EXPERIMENTS AND [9]'S EXPERIMENTS.

Exp #	Number of test samples	Detected		False negative N#(rate)	False positive N#(rate)	Success rate
		without skipping	with skipping			
1 st (ours)	800	738	52	8 (1%)	2 (0.25%)	98.75%
2 nd (ours)	335	297	30	6 (1.79%)	2 (0.59%)	97.61%
1&2(ours)	1135	1035	82	14 (1.23%)	4 (0.35%)	98.41%
1 st [9]	335		333	2 (0.6%)	45 (13.43%)	99.4%
2 nd [9]	448		441	7 (1.5%)	54 (12.05%)	98.4%

Although the detection rate in 1st[9] is higher than in 2nd(ours), we have less FP rate (0.25%) compared to (13.4%). In addition, the output of our system is at the second stage of LP recognition systems (symbol segmentation stage), which implies that the error percentage in [9] will increase after performing the symbol segmentation stage. Moreover, the method in [9] used 89 random samples from 335 samples to adapt the system which can be considered as training samples that are used again in the test phase. In our case, only one sample (outside of test dataset) is required to construct the GRM matrix, no training is needed. The second experiment performed by the author in [9] was done to prove the ability of his system to detect larger LPs, which resulted in extra 5 undetected samples (after adding 113 samples), which means that the system accuracy is affected by scaling. In our case, scaling, will not affect the results if done on the same dataset as long as the candidate symbols lie within the specified ranges in the size filtering stage. This can be verified from the results of our first experiment where symbol heights ranges from 16 to 300 pixels. Also, we can deduce that the system in [9] is resolution dependent because all images were scaled to 640x480 before performing the experiments. However, the following samples of images reveal the robustness and distinction of our approach. Samples from the first set of images in experiment 1 are shown in table V and samples from the second set in experiment 2 are shown in table VI and VII. The real number below each image indicates the objective distance value according to the input prototype GRM for each experiment. The maximum accepted value of the OD for both experiments is 8 (increased to 15 to show cases –some of them are outside the test samples- having physical or perspective distortion or blurring due to movement of the capturing device). Table VII includes samples categorized as in [35]. The shown images include the following difficulties:

- Different resolution, scaling, different perspective distortion and different plate locations for all images in both experiments.

- Different illumination conditions at day and night with
 - Poor ambient lighting: Table V: E1, E2, E3, E4, and Table VI: B1, D5.
 - Blurred images: Table V: A2, B3, B4, C2, C3, C4, C5, D5, D6 and Table VI: B4, E4, G4.
 - Shadows: Table V: A2, A3, A4, A5, B4, D4, H1 and Table VI: B2, B3, C2, C4, D4, F1.
 - Low contrast: Table V: B2, D2 and Table VI: A1, C1, C2, D3, F2.
 - Strong headlight, back light or high flash influences: Table V: F1, F2, F3, F4, F5 and Table VI: G2, G4.
- Plate distortion: Table V: A1, B1, C1, C2, C3, C4, C5, C6, E5 and Table VI: A1, A2, A4, D3, E1, F1.
- Aging effects: Table V: A1, B1, E5, E6, H5, H6, G5, F6 and Table VI: A1, A2, C3, F3.
- Pictures cluttered with :
 - Texture regions (inside or outside the vehicle): Table V: A3, E6, H1, H2, H3, H5 and Table VI: A5, C4, D5, E3, F1, F2, F3, G1, G3.
 - Edge regions (inside or outside the vehicle): Table V: A1, B4, E5, H4, H6, and Table VI: C1, D1, F4, G3.
 - Different objects in the background: Table V: A3, C4, D4, H2 and Table VI: A3, C1, C2, C4, E2, F3, F5, G5.
- Examples of images detected despite the presence of other text similar to the license number's text: Table V: D3, G1, G2, G3, G4, G5 and Table VI: A5, G5.
- Both LP background and vehicle body have the same color: Table V: B2, B5, C3, C4 and Table VI: B3.
- Plate background color is not white: Table VI: D1, D2.
- Touching symbols (detected after skipping modification): Table V: A6, B6, C6, E6, H5 and Table VI: A4, A5, B3, B5, C5, D3, D5, F1.
- Broken or missed symbols (detected after skipping modification): Table V: A1, E5, F6, H6 and table VI: A1, A2, C1, E5, F3.

Regarding the speed of our system, without code optimization and working on a 2.6 GHZ PC with 2 GB RAM, on average 0.12s is needed to locate the LP symbols for low resolution images (640x480) and 0.34s for high resolution images (2048x1536). This non linear relation between speed and resolution is due to other factors that affect the speed of different stages of the system such as the complexity of the image which affects both image processing and GA stages. The character recognition phase is expected to take not more than 0.03s because all symbol images are now available, no further segmentation is required. Hence, 2 to 6 images per second can be fully recognized depending on the resolution and capturing conditions. If we consider the detection speed in [9], which ranges from 39ms to 49.8ms for 640x480 resolution, we will notice that our system is approximately two times slower than [9] but many points should be considered regarding this difference in speed. First, there is an extra time needed to segment the LP into isolated symbols as in our system. Second, the grayscale conversion and size scaling times may not be considered in [9]. Third, the author in [9] didn't mention the programming environment which may be visual C++ or MATLAB. Finally, we believe that enhancing the speed of our system needs further code optimization at many stages.

TABLE V: EXAMPLES OF IMAGES DETECTED IN EXPERIMENT 1 WITH OD VALUES UNDER EACH.

A						
OD	4.7333	3.6721	7.991	4.990	4.629	6.7165
B						
OD	4.275	3.904	4.540	4.401	10.2	5.2428
C						
OD	3.533	6.616	13.95	11.25	4.6652	6.7334
D						
OD	4.6266	6.520	2.0438	3.5995	2.0425	3.701
E						
OD	1.9499	2.594	2.3397	2.7247	3.6925	4.9848
F						
OD	2.6487	2.510	3.3188	1.9581	4.274	5.4282
G						
OD	5.659	2.0717	2.9847	3.1972	6.79	9.29
H						
OD	3.799	3.889	7.727	3.87	5.4284	3.408

TABLE VI: EXAMPLES OF IMAGES DETECTED IN EXPERIMENT 2 WITH OD VALUES UNDER EACH IMAGE.





































A					
OD	5.1661	5.5576	2.918	2.319	4.6923
B					
OD	2.3132	1.9521	3.1722	2.2917	4.4408
C					
OD	2.3132	1.9521	3.1722	2.2917	4.4408
D					
OD	3.1062	3.1632	5.7641	4.155	2.257
E					
OD	2.5	2.6911	5.604	2.529	1.3798
F					
OD	5.288	2.930	1.9917	2.942	4.6444
G					
OD	3.8149	2.9002	2.4042	3.1057	2.9153

TABLE VII: EXAMPLES OF IMAGES DETECTED IN EXPERIMENT 2 AS CLASSIFIED IN [35].

	1	2	3	4	5
Day Large Sample					
OD	1.964	1.590	2.925	3.138	1.870
Day Large Sample					
OD	1.810	3.362	1.433	2.474	4.118
Day Large Sample					
OD	1.766	3.962	2.949	1.899	3.066
DAY Close View					
OD	1.339	1.842	3.734	4.637	2.665
DAY Close View					
OD	5.204	2.843	5.483	2.842	3.079
DAY Close View					
OD	1.486	1.144	2.993	3.983	3.326
DAY with shadow & Shadow in Plate					
OD	2.372	3.958	4.059	3.283	3.166

Considering the genetic phase's speed, great enhancement has been achieved after using the USPS crossover operator. Future research may consider clustering objects according to their sizes and/or positions before being supplied to the genetic phase to allow for the detection of multiple plates and at the same time to increase the system speed. Currently, our system can be used as it is in parking management systems, and in the detection of LPs in pictures taken in emergent circumstances that do not allow adjustment of the position and orientation of the camera with respect to the vehicle. An important point that should be recorded here is that through all the experiments done, we have tried many types of local adaptive thresholding methods, none of them gave 0% error rate but after introducing the skipping part of the genetic phase the error percentage due to binarization has been minimized as shown in the final results. Local adaptive (or dynamic) thresholding has been used a lot but integrating it with CCAT and the skipping GA gives our technique distinction among others. In spite of increasing the computation time of the system, the skipping part in the genetic phase reduces human intervention rate in case of system failure in the detection of some LPs. In other words, more effort should be carried out in the image processing phase to reduce the skipping time while maintaining high accuracy rate of the system.

CONCLUSIONS

A new genetic based prototype system for localizing 2-D compound objects inside plane images has been introduced and tested in the localization of LP symbols. The results were encouraging and a new approach for solving the LP detection problem relying only on the geometrical layout of the LP symbols has been experimentally proved. Also, a flexible system has been introduced that can be simply adapted for any LP layout by constructing its GRM matrix. The system proved to be invariant to object distance (scaling), insensitive with respect to perspective distortion within a reasonable angle interval, and immutable to a large extent to the presence of other types of images in the vehicle background. Due to the independency on color and the adaptive threshold used for binarization, the proposed system possessed high immunity to changes in illumination either temporarily or spatially through the plate area. Furthermore, our experiments proved that although leaving some features in the compound object representation due to the variable nature of the internal objects such as the aspect ratios and the relative widths, a high percentage success rate was achieved with the aid of the adaptability aspect of the GAs. The ability of the system to differentiate between LP text and normal text has been proved experimentally. A very important achievement is overcoming most of the problems arising in techniques based on CCAT by allowing the GA to skip gradually and randomly one or more symbols to reach to an acceptable value of the objective distance. Moreover, an enhancement in the performance of the developed GA has been achieved by applying the new USPS crossover operators, which greatly improved the convergence speed of the whole system. Finally, a new research dimension for GAs has been opened to allow for the detection of multiple plates and even multiple styles in the same image and to increase the performance in terms of speed and memory and to apply the same technique in other problem domains analogous to the LP problem.

Appendix

A TABLE OF 25 LPs FOR 25 COUNTRIES IN THE 5 CONTINENTS.

Virginia	Arizona	California	Victoria	Canada-Ontario
Bosnia	Greece	Great Britain	Denmark	Germany-west
Argentina	Brazil	Chile	Paraguay	Colombia
Egypt	Cameroon	Kenia	Mauritania	Sudan
Albahrain	Dubai	Jordan	Oman	Qatar

ACKNOWLEDGMENT.

This paper was funded by the Deanship of Scientific Research(DSR), King Abdulaziz University, Jeddah, under grant No.(22-611- D1432). The authors, therefore, acknowledge with thanks DSR technical and financial support.

REFERENCES

- [1] Y. Qiu, M. Sun, and W. Zhou, "License Plate Extraction Based on Vertical Edge Detection and Mathematical Morphology," International Conference on Computational Intelligence and Software Engineering, pp. 1-5, 11-13 Dec. 2009.
- [2] A. Ahmadyard and V. Abolghasemi, " Detecting License Plate Using Texture and Color Information," IST 2008, International Symposium on Telecommunications, pp. 804-808, 2008.
- [3] G. Li, R. Yuan, Z. Yang, and X. Huang, "A Yellow License Plate Location Method Based on RGB Model of Color Image and Texture of Plate," Second Workshop on Digital Media and its Application in Museum & Heritages, pp. 42-46, 2007.
- [4] X. Shi, W. Zhao, Y. Shen, and O. Gervasi, "Automatic License Plate Recognition System Based on Color Image Processing," Lecture Notes on Computer Science, Springer-Verlag, vol. 3483, pp.1159-1168, 2005.
- [5] M. Deriche, " GCC License Plates Detection and Recognition Using Morphological Filtering and Neural Networks," Int J. on Comp. Sci. and Info Security, IJCSIS, vol. 8, No. 8, pp. 263-269, Dec, 2010.
- [6] O. Villegas, D. Balderrama, H. Domínguez and V. Sánchez, " License Plate Recognition Using a Novel Fuzzy Multilayer Neural Network," International Journal of Computers", Issue 1,vol. 3, 2009.
- [7] S.H. Mohades Kasaei, S.M. Mohades Kasaei and S.A. Monadjemi, "A Novel Morphological Method for Detection and Recognition of Vehicle License Plate," American Journal of Applied Science, vol.6 no.12, pp. 2066-2070, 2009.
- [8] A. Theja, S. Jain, A. Aggarwal and V. Kandavli, "License Plate Extraction Using Adaptive Threshold and Line Grouping," International Conference on Signal Processing Systems (ICSPS), vol.1, no., pp. 211-214, 5-7 July 2010.
- [9] P. Tarabek, "Fast license plate detection based on edge density and integral edge image," International Conference on Applied Machine Intelligence and Informatics (SAMI), pp. 37 - 40, 2012. doi: [10.1109/SAMI.2012.6208994](https://doi.org/10.1109/SAMI.2012.6208994)

- [10] V. Abolghasemi, and A. Ahmadyfard, "A Fast Algorithm for License Plate Detection," International Conference on Visual Information Systems, Springer, Vol. 4781, pp. 468-477, 2007.
- [11] S. Roomi, M. Anitha and R. Bhargavi, "Accurate License Plate Localization," International Conference on Computer, Communication & Electrical Technology, 2011, pp. 92-99.
- [12] W. Wang, Q. Jiang, X. Zhou, and W. Wan, "Car License Plate Detection Based on MSER," In Proc. International Conference on Consumer Electronics, Communications and Networks, pp. 3973-3976, 2011.
- [13] H. W. Lim and Y. H. Tay, "Detection of License Plate Characters in Natural Scene with MSER and SIFT Unigram Classifier," In Proc. IEEE Conference on Sustainable Utilization and Development in Engineering and Technology, pp. 95-98, 2010.
- [14] H. Anoual, S. Fkihi, A. Jilbab, and D. Aboutajdine, "Vehicle License Plate Detection in Images," International Conference on Multimedia Computing and Systems, pp. 1-5, 2011.
- [15] X., Zhang, and S. Zhang, "A Robust License Plate Detection Algorithm Based on Multi-Features," International Conference on Computer and Automation Engineering, vol. 5, pp. 598-602, 2010.
- [16] D., Zheng, Y. Zhao and J. Wang, "An Efficient Method of License Plate Location," Pattern Recognition Letters, vol. 26 no.15, pp. 2431-2438, 2005.
- [17] J. Xu, S. Li, and M. Yu, "Car License Plate Extraction Using Color and Edge Information," Machine Learning and Cybernetics, 2004, vol. 6, pp. 3904-3907.
- [18] S. Z. Wang and H. M. Lee, "Detection and Recognition of License Plate Characters With Different Appearances," Proc. Conf. Intell. Transp. Syst., vol. 2, pp.979 -984, 2003.
- [19] L. Carrera, M. Mora, J. Gonzalez and F. Aravena, "License Plate Detection Using Neural Networks," In Proceedings of IWANN vol.2, pp. 1248-1255, 2009.
- [20] M. I. Chacon and A. Zimmermann, "License Plate Location Based on a Dynamic PCNN Scheme," Proc. Int. Joint Conf. Neural Netw., vol. 2, pp.1195 -1200, 2003.
- [21] S.-L. Chang, L.-S. Chen, Y.-C. Chung, and S.-W. Chen, "Automatic License Plate Recognition," IEEE Trans. Intell. Transp. Syst., vol. 5, no. 1, pp. 42 -53, 2004.
- [22] S. K. Kim, D. W. Kim and H. J. Kim "A Recognition of Vehicle License Plate Using a Genetic Algorithm Based segmentation," Proc. Int. Conf. Image Process., vol. 1, pp. 661-664, 1996.
- [23] J. Xiong, S. Du, D. Gao and Q. Shen, "Locating Car License Plate Under Various Illumination Conditions Using Genetic Algorithm," Proc. ICSP, vol.3, pp. 2502 -2505, 2004.
- [24] Z. Ji-yin, Z. Rui-rui, L. Min and L. Yinin, " License Plate Recognition Based on Genetic Algorithm," International Conference on Computer Science and Software Engineering, vol. 1, pp. 965-968, Dec. 2008.
- [25] V. P. de Araújo, R. D. Maia, M. F. S. V. D'Angelo and G. N. R. D'Angelo, "Automatic Plate Detection Using Genetic Algorithm," Proceedings of the 6th WSEAS International Conference on Signal, Speech and Image Processing, pp. 43-48, Sep. 2006.
- [26] K. I. Kim, K. Jung, J. H. Kim, S.-W. Lee and A. Verri, "Color Texture-Based Object Detection: An Application to License Plate Localization," Lecture Notes on Computer Science, Springer-Verlag, vol. 2388, pp. 293-309, 2008.
- [27] J. Cano and J. C. Perez-Cortes, "Vehicle License Plate Segmentation in Natural Images," Lecture Notes on Computer Science, Springer-Verlag, vol. 2652, pp.142-149, 2003.
- [28] M. Sezgin and B. Sankur, "Survey Over Image Thresholding Techniques and Quantitative Performance Evaluation," Journal of Electronic Imaging, vol. 13, pp. 146-165, 2004.
- [29] N. Otsu, "A Threshold Selection Method From Gray Level Histograms," IEEE Trans. Syst., Man, Cybern., vol. 9, no. 1, pp. 62-66, Jan.1979.
- [30] S. E. Umbaugh, Computer Vision and Image Processing, Prentice Hall, New Jersey, 1998, pp. 133-138.
- [31] J. E. Baker, "Reducing Bias and Inefficiency in the Selection Algorithm," International Conference on Genetic Algorithms and their application, pp. 14-21, 1987.
- [32] Z. H. Ahmed, "Genetic Algorithm for the Traveling Salesman Problem Using Sequential Constructive Crossover," International Journal of Biometrics & Bioinformatics, vol. 3, pp. 96-105, 2010.
- [33] W. Lenders, and C. Baier, "Genetic Algorithms for Variable Ordering Problem of Binary Decision Diagrams," Lecture Notes in Computer Science, Springer-Verlag, New York, vol. 3469, pp. 1-20, 2005.
- [34] G. E. Liepins and M. R. Hilliard, "Genetic Algorithms: Foundations and Applications," Annals of Operations Research, 21 (1-4) .pp. 31-58, 1989.
- [35] Medialab Web site, (2012, DEC, 9). [Car Images]. Available: <http://www.medialab.ntua.gr/research/LPRdatabase.html>.



G. Abo Samra received the B.S., M. S., and Ph.D degrees from the faculty of Engineering in Cairo University, Egypt in 1983, 1988, and 1992, respectively, in electronic and communication engineering. He is currently an associate professor at the faculty of Computing and Information Technology, King Abdulaziz University-Saudi Arabia. His research interests include image processing, data hiding, OCR, intelligent transportation systems, pattern recognition, soft computing and computer vision. His research has been supported by the Deanship of Scientific Research (DSR), King Abdulaziz University and King Abdulaziz City for Sciences and Technology.



F. Khalefah is a lecturer in the Faculty of Computing and Information Technology, King Abdulaziz University-Saudi Arabia. His research interests include image processing and pattern recognition. His research has been supported by the Deanship of Scientific Research (DSR), King Abdulaziz University.